J|A|C|S
ARTICLES
Published on Web 03/07/2007

Single-Molecule Spectroscopic Investigation of Energy Migration Processes in Cyclic Porphyrin Arrays

Mira Park,[†] Min-Chul Yoon,[†] Zin Seok Yoon,[†] Takaaki Hori,[‡] Xiaobin Peng,[‡] Naoki Aratani,[‡] Jun-ichi Hotta,[§] Hiroshi Uji-i,[§] Michel Sliwa,[§] Johan Hofkens,*[,§] Atsuhiro Osuka,*[,‡] and Dongho Kim*[,†]

Contribution from the Center for Ultrafast Optical Characteristics Control and Department of Chemistry, Yonsei University, Seoul 120-749, Korea, Department of Chemistry, Graduate School of Science, Kyoto University, Sakyo-ku, Kyoto 606-8502, Japan, and Department of Chemistry, Katholieke Universiteit Leuven, Celestijnenlaan 200F, 3001 Heverlee, Belgium

Received August 10, 2006; Revised Manuscript Received January 11, 2007; E-mail: dongho@yonsei.ac.kr; osuka@kuchem.kyoto-u.ac.jp; johan.hofkens@chem.kuleuven.be

Abstract: Covalently linked cyclic porphyrin arrays have been synthesized to mimic natural light-harvesting apparatuses and to investigate the highly efficient energy migration processes occurring in these systems for future applications in molecular photonics. To avoid an ensemble-averaged picture, we performed a single-molecule spectroscopic study on the energy migration processes of cyclic porphyrin arrays and a linear model compound embedded in a rigid polymer matrix by recording fluorescence intensity trajectories, by performing coincidence measurements, and by doing wide-field defocused imaging. Our study demonstrates efficient energy migration within the cyclic porphyrin arrays at the single-molecule level. By comparison with the data of the linear model compound, we could pinpoint the role of the dipole−dipole coupling between diporphyrin subunits and the rigidity of the cyclic structures on the energy transfer processes.

Introduction

A variety of covalently linked and self-assembled cyclic porphyrin arrays have been envisaged as artificial light-harvesting apparatuses for applications in molecular photonics[1,2] because of their similarities in architecture and subunit structures to the natural photosynthetic LH1 and LH2 complexes, in which energy migration occurs very efficiently.[3−5] One of the contributing factors for the extremely rapid energy migration within cyclic assemblies in natural light-harvesting complexes has been suggested to be the highly symmetric ring structure adopted by the dimer subunits.[5−7] Therefore, the challenge has been to develop synthetic cyclic molecular architectures with an energy migration efficiency similar to that of the natural systems.

Various synthetic strategies have been followed to devise such artificial light-harvesting systems with well-defined and rigid molecular structures, including porphyrin arrays coupled by various linkers. While self-assembly is advantageous for the expansion into larger arrays, the overall structures lack rigidity. The covalent linkage between porphyrin units in a cyclic form can provide an increased rigidity as well as a precise control in overall structure. In this regard, we have prepared a wheel-like structure, the dodecameric porphyrin wheel **C12Z**, and a linear model structure, namely, the dodecameric porphyrin linear array **L12Z**. Both compounds are composed of *meso*−*meso*-linked diporphyrin **Z2** subunits. We also synthesized a tetracosameric porphyrin wheel **C24Z** compound with tetraporphyrin **Z4** subunits, bridged by 1,3-phenylene linkers (Chart 1).[8,9]

[†] Yonsei University.
[‡] Kyoto University.
[§] Katholieke Universiteit Leuven.

(1) (a) Anderson, S.; Anderson, H. L.; Sanders, J. K. M. *Acc. Chem. Res.* **1993**, *26*, 469. (b) Gust, D.; Moore, T. A.; Moore, A. L. *Acc. Chem. Res.* **2001**, *34*, 40. (c) Holten, D.; Bocian, D. F.; Lindsey, J. S. *Acc. Chem. Res.* **2002**, *35*, 57. (d) Kim, D.; Osuka, A. *Acc. Chem. Res.* **2004**, *37*, 735. (e) Imamura, T.; Fukushima, K. *Coord. Chem. Rev.* **2000**, *198*, 133. (f) Satake, A.; Kobuke, Y. *Tetrahedron* **2005**, *61*, 13. (g) Wojaczynski, J.; Latos-Grazynski, L. *Coord. Chem. Rev.* **2000**, *204*, 113. (h) Iengo, E.; Zangrando, E.; Alessio, E. *Eur. J. Inorg. Chem.* **2003**, 2371.
(2) (a) Anderson, H. L.; Sanders, J. K. M. *J. Chem. Soc., Chem. Commun.* **1989**, 1714. (b) Biemans, H. A. M.; Rowan, A. E.; Verhoeven, A.; Vanoppen, P.; Latterini, L.; Foekema, J.; Schenning, A. P. H. J.; Meijer, E. W.; de Schryver, F. C.; Nolte, R. J. M. *J. Am. Chem. Soc.* **1998**, *120*, 11054. (c) Li, J.; Ambroise, A.; Yang, S. I.; Diers, J. R.; Seth, J.; Wack, C. R.; Bocian, D. F.; Holten, D.; Lindsey, J. S. *J. Am. Chem. Soc.* **1999**, *121*, 8927. (d) Drain, C. M.; Nifiatis, F.; Vasenko, A.; Batteas, J. D. *Angew. Chem., Int. Ed.* **1998**, *37*, 2344. (e) Brodard, P.; Matzinger, S.; Vauthey, E.; Mongin, O.; Papamicaël, C.; Gossauer, A. *J. Phys. Chem. A* **1999**, *103*, 5858. (f) Takahashi, R.; Kobuke, Y. *J. Am. Chem. Soc.* **2003**, *125*, 2372. (g) Kato, A.; Sugiura, K.; Miyasaka, H.; Tanaka, H.; Kawai, T.; Sugimoto, M.; Yamashita, M. *Chem. Lett.* **2004**, *33*, 578. (h) Prodi, A.; Chiorboli, C.; Scandola, F.; Iengo, E.; Alessio, E.; Dobrawa, R.; Würthner, F. *J. Am. Chem. Soc.* **2005**, *127*, 1454.
(3) McDermott, G.; Prince, S. M.; Freer, A. A.; Hawthonthwaite-Lawless, A. M.; Papiz, M. Z.; Cogdell, R. J.; Isaacs, N. W. *Nature* **1995**, *374*, 517.
(4) Sundström, V.; Pillerits, T.; van Grondelle, R. *J. Phys. Chem. B* **1999**, *103*, 2327.
(5) (a) Gensch, T; Hellingwerf, K. J.; Braslavsky, S. E.; Schaffner, K. *J. Phys. Chem.* **1998**, *102*, 5398. (b) van Oijen, A. M.; Ketelaars, M.; Köhler, J.; Aartsma, T. J.; Schmidt, J. *Science* **1999**, *285*, 400.
(6) Karrasch, S.; Bullough, P. A.; Ghosh, R. *EMBO J.* **1995**, *14*, 631.
(7) Bradforth, S. E.; Jimenez, R.; van Mourik, F.; van Grondelle, R.; Fleming, G. R. *J. Phys. Chem.* **1995**, *99*, 16179.
(8) Peng, X.; Aratani, N.; Takagi, A.; Matsumoto, T.; Kawai, T.; Hwang, I.-W.; Ahn, T. K.; Kim, D.; Osuka, A. *J. Am. Chem. Soc.* **2004**, *126*, 4468.
(9) Hori, T.; Aratani, N.; Takagi, A.; Matsumoto, T.; Kawai, T.; Yoon, M.-C.; Yoon, Z. S.; Cho, S.; Kim, D.; Osuka, A. *Chem.—Eur. J.* **2006**, *12*, 1319.

Chart 1. Molecular Structures of Linear Array **L12Z** (a), *meso*−*meso* Directly Linked Zn(II) Diporphyrin **Z2** and Dodecameric Porphyrin Wheel **C12Z** (b), and Tetraporphyrin **Z4** and Tetracosameric Porphyrin Wheel **C24Z** (c)[a]

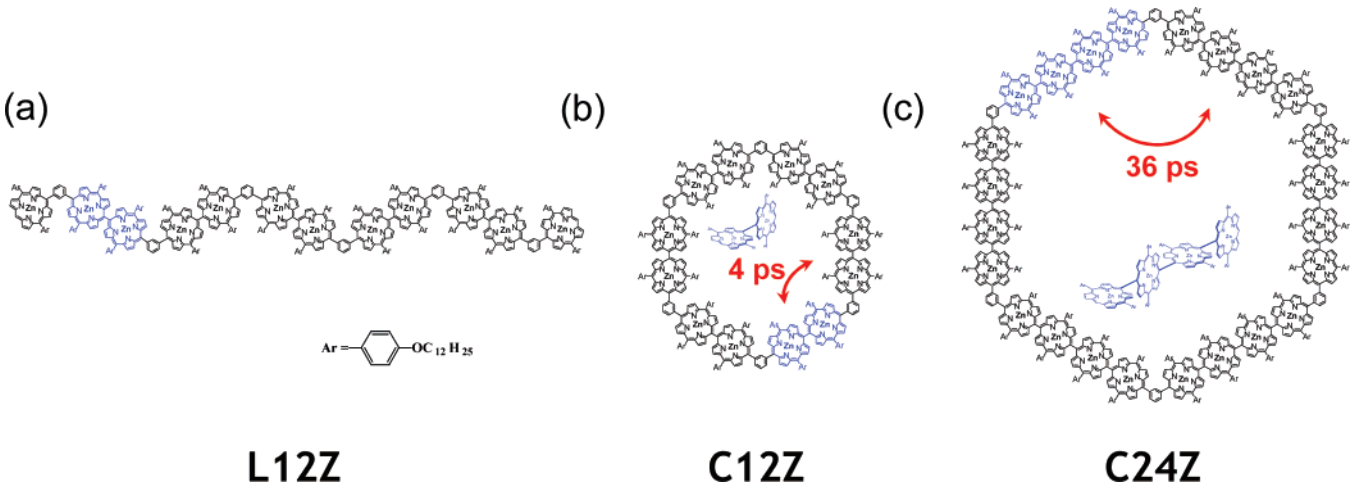

[a] In an ensemble study, ∼4 and ∼36 ps for **C12Z** and **C24Z**, respectively, have been assigned to the excitation energy migration time between *meso*−*meso* directly linked diporphyrins and tetraporphyrins.

In this study, the energy migration processes in **C12Z** and **C24Z** are comparatively investigated by single-molecule spectroscopy (SMS) with a particular focus on the influences of (1) the coupling strength between porphyrin subunits and (2) the rigidity of the structure on the energy migration efficiency using fluorescence intensity trajectories (FITs), coincidence measurements,[10−14] and wide-field defocused imaging.[15,16] Since spectroscopic investigations at the single-molecule level (SMS) eliminate the averaging effect inherent in ensemble spectroscopic measurements, SMS can provide information on individual molecular behavior hidden in ensemble measurements.

Experimental Section

Sample Preparation and Steady-State Spectroscopic Measurements. The details on the synthesis of linear and cyclic porphyrin arrays studied here were documented in several previous papers.[8,9] Steady-state absorption spectra were recorded by using a UV−vis spectrometer (Varian, model Cary5000). Samples for single-molecule measurements were prepared by spin-coating (2000 rpm) of a solution of a zinc(II) porphyrin array (∼10^{-10} M) in chloroform (Aldrich, spectrophotometric grade) containing 2−5 mg/mL poly(methyl methacrylate) (PMMA) on rigorously cleaned cover glasses. The optical density of the sample solution was measured to determine the concentration.

Instrumentation. Fluorescence at the single-molecule level was measured by using laser scanning confocal and wide-field microscope systems based on an inverted type optical geometry. For coincidence measurements, a classical Hanbury-Brown and Twiss type coincidence setup[10] was used in combination with pulse laser excitation. As an excitation light source (568 nm, repetition rate 8.18 MHz, 1.2 ps full width at half-maximum), the output of a frequency-doubled OPO, pumped by a Ti:sapphire oscillator (800 nm, Tsunami, Spectra Physics), and a pulse picker were used. The excitation light was focused by an objective lens (Olympus, 1.4 NA, 100×) on the sample. For coincidence measurements and FITs, we have used the same picosecond pulse laser (568 nm) as an excitation light source. For both measurements, the fluorescence from a single molecule was collected by the same objective and split by a 50/50 nonpolarizing beam splitter and the emitted photons were detected by two avalanche photodiodes (APD, SPCM-AQR-15, Perkin-Elmer Optoelectronics, Norwalk, CT); one was connected to the router directly and the other to the router after a delay generator to compensate for the dead time of the SPC board (SPC630, Becker and Hickl). The signal was acquired using the first-in−first-out mode in which the arrival time after the beginning of acquisition, the time delay between the start and stop pulses, and the detection channels (APD1 or APD2) are registered for each detected fluorescence photon. The central peak at a delay time of 0 ns in the distribution of interphoton arrival times corresponds to photon pairs generated from the same laser pulse. In all other cases, interphoton arrival times are distributed around a multiple of the laser repetition period (every 123 ns, lateral peaks). For wide-field defocused imaging, the 488 nm cw beam from an Ar ion laser was focused onto the back focal plane of the objective lens to achieve a maximum homogeneous wide-field illumination of the sample. Imaging was performed with slight defocusing of the optics, and the circular polarization of the excitation light was achieved by using a polychromatic Fresnel rhomb (FR600QM, Thorlab). The fluorescence was collected by the same objective, passed through a dichroic mirror and long-pass filters, and then imaged onto an EMCCD camera (Cascade 1, Roper Scientific). The orientation of the emission dipole was obtained by fitting the experimental defocused images with patterns, calculated via wave-optical expressions. Note that different excitation wavelengths were used for defocused wide-field defocused imaging (488 nm) and coincidence measurements and FITs (568 nm). Excitation at 488 nm results in excitation in the S_2 band, which is followed in these compounds by fast internal conversion to the S_1 band. As a result, the same excited state is probed in both excitation conditions (see the Supporting Information, p 1).

Results and Discussion

Ensemble Spectroscopy. In ensemble measurements, a comparison of the absorption spectra of **C12Z**[8] and **C24Z**[9] with those of their respective building blocks, **Z2** and **Z4**, reveals that the dipole−dipole coupling is stronger in **C12Z** due to the

(10) Hanbury-Brown, R.; Twiss, R. Q. *Nature* **1956**, *177*, 27.
(11) Masuo, S.; Vosch, T.; Cotlet, M.; Tinnefeld, P.; Habuchi, S.; Bell, T. D. M.; Oesterling, I.; Beljonne, D.; Champagne, B.; Müllen, K.; Sauer, M.; Hofkens, J.; De Schryver, F. C. *J. Phys. Chem. B* **2004**, *108*, 16686.
(12) Tinnefeld, P.; Müller, C.; Sauer, M. *Chem. Phys. Lett.* **2001**, *345*, 252.
(13) Weston, K. D.; Dyck, M.; Tinnefeld, P.; Müller, C.; Herten, D. P.; Sauer, M. *Anal. Chem.* **2002**, *74*, 5342.
(14) Tinnefeld, P.; Weston, K. D.; Vosch, T.; Cotlet, M.; Weil, T.; Hofkens, J.; Müllen, K.; De Schryver, F. C.; Sauer, M. *J. Am. Chem. Soc.* **2002**, *124*, 14310.
(15) Bartko, A. P.; Dickson, R. M. *J. Phys. Chem. B* **1999**, *103*, 11237.
(16) Schroeyers, W.; Vallée, R.; Patra, D.; Hofkens, J.; Habuchi, S.; Vosch, T.; Cotlet, M.; Müllen, K.; Enderlein, J.; De Schryver, F. C. *J. Am. Chem. Soc.* **2004**, *126*, 14310.

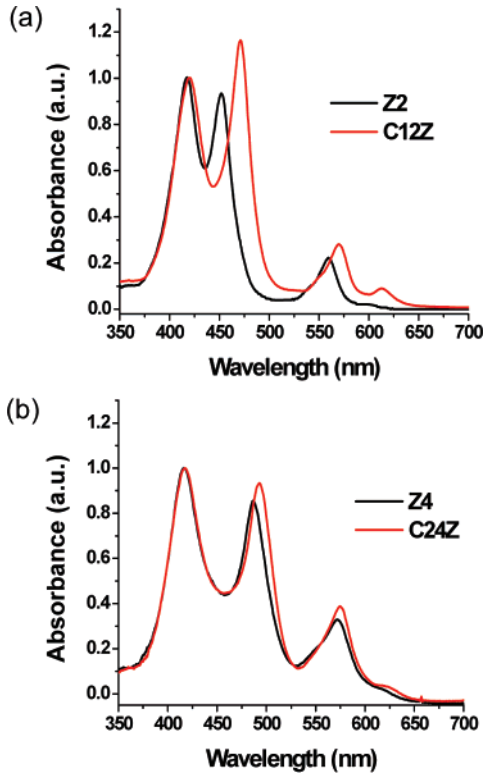

Figure 1. Absorption spectra of **Z2** and dodecameric porphyrin wheel **C12Z** (a) and **Z4** and tetracosameric porphyrin wheel **C24Z** (b). The concentrations are in the range of 5×10^{-6} M.

shorter interchromophoric distance between **Z2** subunits despite the weaker transition dipole strength in **Z2** than that in **Z4**.[17,18]

The absorption spectrum of **C12Z** clearly shows the signature of relatively strong coupling between diporphyrin subunits **Z2** as compared with that of its constituent unit, **Z2**. Indeed, a spectral red shift can be observed when the spectra of **C12Z** and **Z2** are compared. On the other hand, the absorption spectrum of **C24Z** is very similar to that of the tetraporphyrin subunit **Z4**, indicating a rather weak coupling between tetraporphyrins due to the longer interchromophoric distance. More quantitatively, we calculated the dipole−dipole coupling strength to investigate the interactions among **Z2**s in **C12Z** and **Z4**s in **C24Z**, which corresponds to the optical red shift in the steady-state absorption spectra (Figure 1). In this calculation, we assumed that the array-axis transition dipole in **Z2** would be the origin of the low-energy B-band, and its magnitude was estimated to be 19 D from the absorption spectrum. Parameters for the calculation include information on the relative orientation of the transition dipoles, the distance between the transition dipoles, and the dielectric constant of the solvent. As a result, the interaction matrix can be obtained, and each element in the square matrix is the coupling energy between the two adjacent transition dipoles in **C12Z** and **C24Z**. The dipole coupling energies between the neighboring subunits, **Z2**s in **C12Z** and **Z4**s in **C24Z**, respectively, were calculated to be 943 and 38 cm^{-1} in the B-band and 140 and 11 cm^{-1} in the Q-band by diagonalization of the matrix with coupling energies.[18] Thus, according to the Förster-type incoherent energy transfer theory based on the dipole−dipole coupling strength, we can expect that the energy migration process in **C12Z** is faster than that in **C24Z**. On the basis of the transient absorption anisotropy decay in ensemble measurements,[8,9,17] we have obtained energy migration times of ∼4 and ∼36 ps for **C12Z** and **C24Z**, respectively. In addition, for the large cyclic array **C24Z**, the energy migration time (∼36 ps) is similar to that of the bichromophoric model compound **2Z4** (∼33 ps; see the Supporting Information, p 2). In contrast, the energy migration time of **C12Z** (∼4 ps) is about 2 times faster than that of its bichromophoric model compound **2Z2** (∼9 ps; see the Supporting Information, p 1). The difference in the energy migration times between the cyclic arrays **C12Z** and **C24Z** and their corresponding model compounds **2Z2** and **2Z4** (Supporting Information, p 2) indicates that conformational heterogeneity exists in **C24Z**. Moreover, we observed an intensity-dependent decay component in the transient absorption temporal profiles indicative of singlet−singlet (S_1-S_1) annihilation processes occurring in **C12Z** and **C24Z**.[8,17−19]

Single-Molecule Fluorescence Intensity Traces. Under atmospheric conditions, the FITs of single molecules of the reference linear array **L12Z** and cyclic arrays **C12Z** and **C24Z** exhibit structure-dependent behavior. The fluorescence quantum yields of the linear and cyclic porphyrin arrays determined in ensemble measurements were very low ($\Phi_f < 0.1$). Hence, it can be easily understood that bin times of at least 50 ms have to be used to achieve a sufficient signal-to-noise ratio in the FITs. This also means that it is impossible to obtain information on processes occurring on time scales faster than 50 ms from the FITs.[20] In FITs, off times can be induced by several dynamical processes such as the triplet-state population, conformational changes, and molecular rotation.[22−24] We cannot observe the off times induced by the triplet-state population because the triplet-state lifetimes (microseconds to milliseconds) in immobilized single molecules are shorter than the bin time (50 ms).[21,22] Molecular rotation as a source for long off times can be ruled out due to the high glass transition temperature of PMMA used (T_g = 122 °C) and large size of the porphyrin wheels, especially taking into account the long side chains in the porphyrin arrays.

For **Z2**, the subunit of **L12Z** and **C12Z**, and for **Z4**, the subunit of **C24Z**, the FITs exhibit two or four stepwise photobleaching behaviors, respectively, without long off times as shown in the Supporting Information, p 3. The representative FITs of **L12Z** exhibit clearly longer off times than those of the two cyclic arrays (Figure 2, Supporting Information, p 4). Long off times have been seen in the FITs of many different immobilized single molecules and have recently been associated with spurious electron transfer to or from the matrix.[25−30] The FITs of 39 **L12Z** molecules were analyzed, and an average off

(17) Hwang, I.-W.; Ko, D. M.; Ahn, T. K.; Yoon, Z. S.; Kim, D.; Peng, X.; Aratani, N.; Osuka, A. *J. Phys. Chem. B* **2005**, *109*, 8643.
(18) Yoon, Z. S; Yoon, M.-C.; Kim, D. J. *Photochem. Photobiol., C* **2005**, *6*, 249.
(19) De Belder, G.; Schweitzer, G.; Jordens, S.; Lor, M.; Mitra, S.; Hofkens, J.; De Feyter, S.; Van der Auweraer, M.; Herrmann, A.; Weil, T.; Müllen, K.; De Schryver, F. C. *ChemPhysChem* **2001**, *2*, 49.
(20) Piwonski, H.; Stupperich, C.; Hartschuh, A.; Sepiol, J.; Meixner, A.; Waluk, J. *J. Am. Chem. Soc.* **2005**, *127*, 5302.
(21) Yip, W.-T.; Hu, D.; Vanden Bout, D. A.; Barbara, P. F. *J. Phys. Chem. A* **1998**, *102*, 7564.
(22) Köhn, F.; Hofkens, J.; Gronheid, R.; Van der Auweraer, M.; De Schryver, F. C. *J. Phys. Chem. A* **2002**, *106*, 4808.
(23) Hou, Y.; Higgins, D. A. *J. Phys. Chem. B* **2002**, *106*, 10306.
(24) Deschenes, L. A.; Vanden Bout, D. A. *Science* **2001**, *292*, 255.
(25) Yeow, E. K. L.; Melnikov, S. M.; Bell, T. D. M.; De Schryver, F. C.; Hofkens, J. *J. Phys. Chem. A* **2006**, *110*, 1726.
(26) Haase, M.; Hübner, C. G.; Reuther, E.; Herrmann, A.; Müllen, K.; Basché, Th. *J. Phys. Chem. A* **2004**, *108*, 10445.

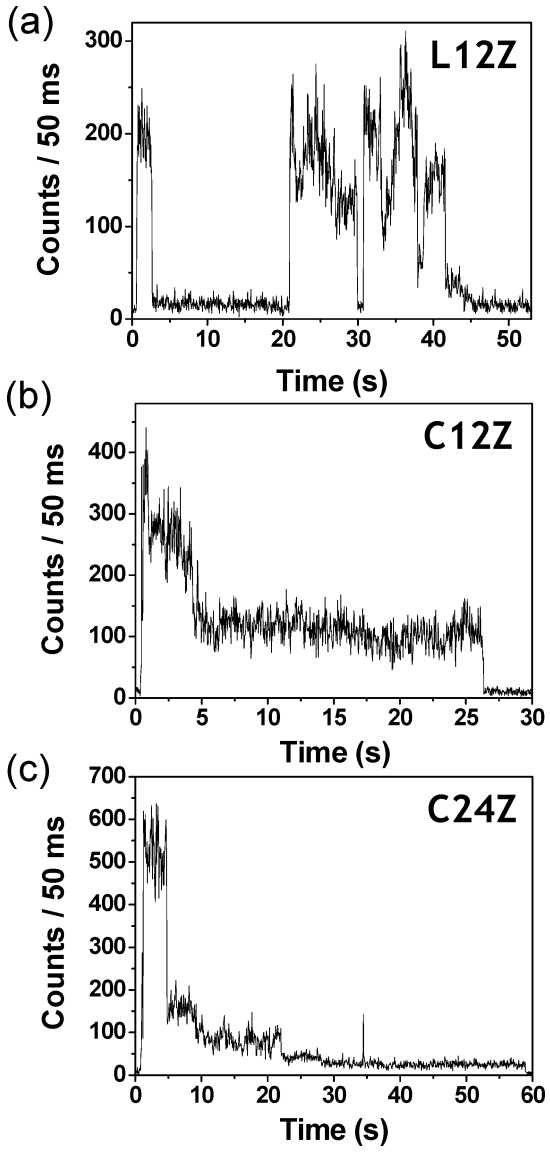

Figure 2. Fluorescence intensity trajectories of 1,3-phenylene-bridged Zn(II) porphyrin linear array **L12Z** (a) and cyclic arrays **C12Z** (b) and **C24Z** (c) embedded in a PMMA polymer matrix.

time of several seconds was obtained in 56% of the investigated FITs. In contrast, in only 27% and 25% of the investigated FITs of 63 **C12Z** molecules and 56 **C24Z** molecules, respectively, off times of several seconds were seen. Since **C12Z** and **L12Z** are composed of the same building blocks, a difference in redox properties cannot account for the different occurrences of long off times (assuming that spurious electron transfer is also involved in the long off state here). The frequent occurrences of long off times in **L12Z** could eventually be explained in terms of the existence of nonradiative decay channels, induced by the more flexible conformation of **L12Z**, which leads to more frequent kink structures.[31,32] Such conformational flexibility is

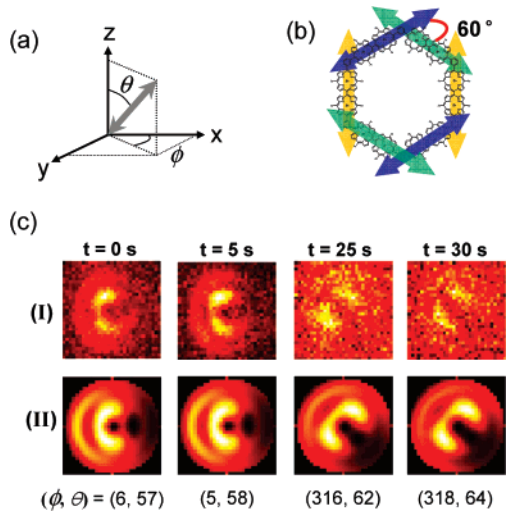

Figure 3. Definition of angles: ϕ indicates the in-plane (in the *xy* plane) angle, and θ indicates the out-of-plane angle (inclination angle between the optical dipole (bold arrow in gray) and excitation optical axis (*z* axis)) (a). Model with observed dipole moments (colored arrows) in **C12Z** (b). Snapshots of experimentally observed emission patterns of **C12Z** (sequence I) and corresponding calculated patterns (sequence II) as a function of time (c).

significantly reduced in the cyclic arrays, which exhibit a well-defined orientation of diporphyrin subunits. In good agreement with this hypothesis, the FITs of **C12Z** and **C24Z** show a lower occurrence of off times and a stepwise photobleaching behavior, indicating more efficient energy migration in these compounds compared with the **L12Z** linear array (vide infra) under identical excitation conditions (Figure 2). Indeed, the stepwise photobleaching detected in **C12Z** and **C24Z** is similar to the behavior seen in FITs of other multichromophoric compounds at the single-molecule level.[31−34] Hence, the model proposed for these systems, involving one of the chromophores acting as a fluorescent trapping site and energy migration toward this trapping site in combination with temporal evolution of the trapping site due to photobleaching, can be claimed here as well. This observation fits well with the ensemble data that indicate more efficient energy migration in the cyclic arrays as compared to the linear array.[17,31] Note that the detailed mechanism that links the higher conformational flexibility of **L12Z** to spurious electron transfer induced long off states still needs to be unraveled.

Wide-Field Defocused Imaging. To explain the stepwise photobleaching pattern observed in the FITs of the cyclic compounds, we have proposed a model involving one fluorescent trapping site that is dynamic as a function of time. If this is true, we should be able to determine the orientation of this trapping site. It has been demonstrated that the orientation of the emitting trapping site of a single molecule embedded in a polymer film can be determined by wide-field defocused imaging.[15,16] The characteristic intensity distribution of the defocused images allows for the determination of the 3-dimensional emission dipole orientation. There are six emitting dipoles in **C12Z** as shown in Figure 3b.

(27) Schuster, J.; Cichos, F.; von Borczyskowski, C. *Opt. Spectrosc.* **2005**, *98*, 778.
(28) Schuster, J.; Cichos, F.; von Borczyskowski, C. *Appl. Phys. Lett.* **2005**, *87*, 051915.
(29) Zondervan, R.; Kulzer, F.; Orlinskii, A. B.; Orrit, M. *J. Phys. Chem. A* **2003**, *107*, 6770.
(30) Hoogenboom, J. P.; van Dijk, E. M. H. P.; Hernando, J.; van Hulst, N. F.; García-Parajó, M. F. *Phys. Rev. Lett.* **2005**, *95*, 097401.
(31) Park, M.; Cho, S.; Yoon, Z. S.; Aratani, N.; Osuka, A.; Kim, D. *J. Am. Chem. Soc.* **2005**, *127*, 15201.
(32) Becker, K.; Lupton, J. M. *J. Am. Chem. Soc.* **2006**, *128*, 6468.
(33) Hofkens, J.; Maus, M.; Gensch, T.; Vosch, T.; Cotlet, M.; Köhn, F.; Herrmann, A.; Müllen, K.; De Schryver, F. C. *J. Am. Chem. Soc.* **2000**, *122*, 9278.
(34) Bopp, M.; Jia, Y.; Li, L.; Cogdell, R. J.; Hochstrasser, R. M. *Proc. Natl. Acad. Sci. U.S.A.* **1997**, *94*, 10630.

The two emission dipoles facing each other have the same emission pattern due to the symmetry of the molecular system (identical angle ϕ), so a maximum of three differently oriented emitters can be expected. If emission dipoles of the single cyclic array are not in-plane (the *xy* plane), in other words, if the angle θ between the *z* axis and the emission dipole is close to zero, the change in emission patterns cannot be observed clearly.[15,16] In Figure 3c, the porphyrin wheel **C12Z** is tilted by ~30° from the laboratory *xy* plane (i.e., the tilting angle θ from the *z* axis was calculated to be ~60°). The emission patterns of the cyclic array **C12Z** as a function of time are depicted in Figure 3c. As shown in Figure 3c, the experimental emission patterns change as a function of time. As argued before, the molecular rotational motion of **C12Z** is prohibited in the PMMA polymer matrix at room temperature due to the large size of **C12Z** with long side chains and the high T_g of the PMMA used. Thus, the different patterns represent the different porphyrin units in the cyclic array that serve as emissive trapping sites in the time course of the experiment. In this series, we observed only two different patterns, probably because the porphyrin units with different orientations in the cyclic porphyrin array were bleached during alignment or because of the low count rate when the majority of the absorbing/emitting units are bleached. On the basis of fitted patterns, the relative angle between the different emission dipoles was calculated to be ~60°, in excellent agreement with the value expected from the molecular structure. This experiment clearly proves the validity of the model that evokes emissive trapping sites and efficient energy migration toward these trapping sites.

Coincidence Measurements. Coincidence measurements were carried out on single molecules of **L12Z**, **C12Z**, and **C24Z** to identify whether the molecule acts as a single emitter (one photon is emitted per pulse) or not (two or more photons are emitted per pulse) when excited with relatively intense laser pulses.[11−14] This measurement would demonstrate that the S_1-S_1 annihilation process can be observed at the single-molecule level. For coincidence measurements, a classical Hanbury-Brown and Twiss type coincidence setup[10] was used in combination with pulse laser excitation. The excitation laser power of 1.8 μW at the back focal plane of the microscope was employed to increase the probability that two excitons are generated in the porphyrin wheel at the same time. When one fluorescence photon per laser pulse is detected at most, the histogram of interphoton arrival times shows a low occurrence of detected photons at the central peak around 0 ns. In all other cases, interphoton arrival times are distributed around a multiple of the laser repetition period, i.e., one peak every ~123 ns. For two emission photons generated per laser pulse, the central peak has a ratio of 0.5 with respect to multiple lateral peaks.[12,13] The interphoton arrival time distribution of a single **C12Z** molecule shows a typical time pattern with a very small central peak as compared to the two lateral peaks (Figure 4a). The central peak can also be related to a few accidental coincidences, which are attributed to background−background, background−signal, and signal−background photon pairs. The histograms of N_C/N_L ratios (the ratio between the number of events at the central position (N_C) and those at lateral positions (N_L)) for 70 single molecules of **L12Z**, **C12Z**, and **C24Z** are compared in Figure 4b.

The N_C/N_L ratio in the coincidence measurements can be used to estimate the number of emitting porphyrin units in the multichromophoric arrays. The N_C/N_L ratio of the linear array **L12Z** is centered around 0.43 and has a much wider distribution compared with those of the cyclic arrays **C12Z** and **C24Z**. The N_C/N_L value of 0.43 is close to the expected value of 0.5 for a two-photon emitter. This relatively high N_C/N_L value suggests less efficient S_1-S_1 annihilation in the linear array **L12Z**. The larger spread can be explained presumably by the larger conformational heterogeneity. As shown in Figure 2a, the FITs of the linear array **L12Z** show large intensity variations and multiple intensity levels. This might be related to variations in the number of emitters (excited states) simultaneously present in these molecules. At the same time, it indicates that energy hopping as well as S_1-S_1 annihilation is less efficient in the linear array **L12Z** than in the cyclic arrays. Indeed, **C12Z** and **C24Z** exhibit reduced mean N_C/N_L ratios of 0.24 and 0.35, respectively, indicating a more efficient S_1-S_1 annihilation process in **C12Z** than that in **C24Z**. The smaller value of N_C/N_L for **C12Z** than for **C24Z** illustrates that **C12Z** can be considered as a well-defined cyclic structure for Förster resonance energy transfer (FRET) processes due to stronger dipole−dipole coupling between **Z2** subunits. In the case of the larger porphyrin wheel **C24Z**, the longer interchromophoric distance between **Z4** subunits leads to less efficient FRET processes (both hopping or energy migration and singlet−singlet annihilation) than those in **C12Z**. However, the mean N_C/N_L ratio of **C24Z** is lower than that of **L12Z**, although **C24Z** has 2 times the number of porphyrin units as **L12Z**. This can be explained by the fact that excitation energy migration in the cyclic porphyrin array **C24Z** is more efficient than that in the linear porphyrin array **L12Z**. In addition, the overall structure of **C24Z** seems to be less rigid compared with the small and

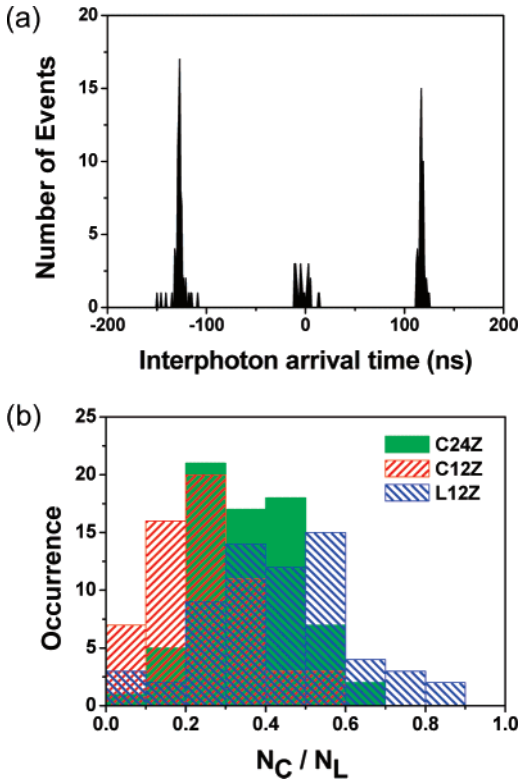

Figure 4. Interphoton arrival time distribution in the coincidence measurements obtained for **C12Z** (a) and the histogram of N_C/N_L values of single **L12Z**, **C12Z**, and **C24Z** molecules (b). The mean values of the N_C/N_L ratios for **L12Z**, **C24Z**, and **C12Z** are 0.43, 0.35, and 0.24, respectively.

rigid cyclic structure of **C12Z** because the wheel structure with **Z4** subunits is slightly distorted as shown in the STM images (Supporting Information, p 5). This geometrical distortion might also reduce the energy migration efficiency by introducing competitive nonradiative decay channels.

Conclusions

We have comparatively investigated the single-molecule fluorescent properties occurring in a linear porphyrin array, **L12Z**, and two cyclic porphyrin arrays, **C12Z** and **C24Z**, to gain further insight into the energy migration processes occurring in these systems. Recording of FITs by means of single-molecule spectroscopy revealed a difference in the efficiency of energy migration processes in **C12Z** and **C24Z** compared with the linear analogue. The relative change in the angle of the orientation of the emissive trapping sites in **C12Z** after photobleaching was observed to be ~60° by wide-field defocused imaging, in excellent agreement with the value expected from the molecular structure. Both measurements confirm that an earlier model describing energy migration in single multichromophoric compounds also holds for the cyclic porphyrin arrays. In addition, the efficiency of the singlet−singlet annihilation process was observed to be different in the linear array and two cyclic arrays as demonstrated by coincidence measurements. The highly efficient energy migration in **C12Z** can be linked to its well-defined rigid structure and relatively strong dipole−dipole interactions between the neighboring subunits. These results will provide useful information for future integration of artificial molecular light-harvesting devices based on cyclic porphyrin arrays in the solid state.

Acknowledgment. This research was financially supported by the Star Faculty Program of the Ministry of Education and Human Resources Development of Korea (D.K.). M.P., M.-C.Y., and Z.S.Y. acknowledge a fellowship of the BK21 program from the Ministry of Education and Human Resources Development. The work at Kyoto was supported by CREST (A.O.). Financial support from the KULeuven research fund (Grant GOA 2/06, Center of Excellence INPAC) and the Federal Science Policy of Belgium (Grants IUAP-V-03 and IUAP-VI) is also acknowledged. This work, as part of the European Science Foundation EUROCORES Program SONS, was supported by funds from the FWO and EC Sixth Framework Program, under Contract No. ERAS-CT-2003-980409.

Supporting Information Available: Five additional figures, with discussion and references. This material is available free of charge via the Internet at http://pubs.acs.org.

JA065813N